Pre-Steady-State Kinetic Characterization of RNA-Primed Initiation of Transcription by HIV-1 Reverse Transcriptase and Analysis of the Transition to a Processive DNA-Primed Polymerization Mode†

Sara H.Thrall,‡,§ Ruth Krebs,‡ Birgitta M. Wöhrl,‡ Luciano Cellai,|| Roger S. Goody,‡ and Tobias Restle*,‡

Max-Planck-Institut für molekulare Physiologie, Abteilung Physikalische Biochemie, Rheinlanddamm 201, 44139 Dortmund, Germany, and Istituto di Strutturistica Chimica, CNR, 00016 Monterotondo Stazione, Rome, Italy

Received May 12, 1998; Revised Manuscript Received July 17, 1998

ABSTRACT: Single-turnover and equilibrium measurements were carried out to determine the basis of the apparently slow, nonprocessive polymerization reaction catalyzed by HIV-1 reverse transcriptase (RT) during transcription initiation, when both the primer and the template are composed of RNA. Comparison of the binding and kinetic parameters of a 20-mer, all-RNA primer/35-mer RNA template substrate to one identical in sequence but composed of a 20-mer, all-DNA primer/35-mer RNA template reveals striking differences. Equilibrium titrations yielded a dissociation constant (K_d) >200 nM for the RNA/RNA−RT complex which is at least 200-fold higher than that of the DNA/RNA−substrate ($K_d \sim 1$ nM). The affinity of the RT−RNA/RNA complex for dTTP was found to be at least 500 times lower ($K_d \sim 3.4$ mM) than that of the RT−DNA/RNA complex ($K_d \sim 6.6\ \mu$M). The single-turnover dNTP incorporation time course using the RNA-primer substrate, the DNA-primer substrate, or a series of RNA-primer substrates preextended with one to eight deoxynucleotides showed that dNTP incorporation occurs with a biphasic exponential burst of +1 extension product, followed by a linear phase. At least three different RT-bound forms of the p/ts exist: a fast, kinetically competent form (single-turnover rate ∼10−50 s^{-1}); a slow form (rate ∼0.3−1 s^{-1}); and a form that is dead-end (no turnover). The studies further revealed that a switch to a fast, kinetically competent p/t occurs after six dNTPs are incorporated into the RNA primer, with the switch being defined as the transition from a minority to a majority of the p/t bound in the optimal manner.

Transcription of the human immunodeficiency virus (HIV)[1] RNA genome by reverse transcriptase (RT) is initiated from a host cell-derived primer, a $tRNA^{Lys3}$ molecule, annealed to the primer binding sequence (PBS) on the viral RNA template (termed the "initiation complex"; for reviews, see *1*, *2*). Many studies have reported an accumulation of short tRNA primer extension products during initiation of (−) strand DNA synthesis, before the appearance of the full-length, strong-stop DNA product (2−5). This transcriptional lag and apparent nonprocessivity during initiation are generally thought to arise from an intricate architecture of RNA secondary structures within and surrounding the initiation complex (*2*, *6*). Ehresmann and co-workers recently probed, by chemical and enzymatic footprinting techniques, the structure of the initiation complex formed by a natural $tRNA^{Lys3}$ molecule annealed to the PBS of a truncated (300 base) HIV RNA template (*7*, *8*). Several secondary structure motifs were detected, including a stem−loop structure located on the viral RNA directly upstream to the 3′-end of the annealed primer, in addition to an interaction between the anticodon loop of the $tRNA^{Lys3}$ with this upstream loop. The resolution of these secondary structures during incorporation of the first few dNTPs onto the tRNA primer could result in the observed nonprocessive polymerization during this time.

Recent studies addressed whether the polymerization mode of the RNA-primed initiation is distinct from that of DNA-primed polymerization which occurs during most of the ∼20 000 dNTP incorporations carried out to synthesize the double-stranded DNA copy of the RNA genome (*5*, *9*). The work showed that the transcriptional pausing occurs during the first 5 dNTP incorporations onto a natural $tRNA^{Lys3}$ primer annealed to the PBS of a truncated (300 base) viral RNA template, before the full-length DNA copy is synthesized. When an 18-mer oligoribonucleotide, or a $tRNA^{Lys3}$ molecule containing no modified bases, was used to prime transcription, the pausing was also observed. Priming of the same viral RNA template by an 18-mer oligodeoxynucleotide, however, resulted in nonpausing, full-length DNA synthesis (*5*, *9*). Evaluation of the incorporation kinetics of two dNTPs onto the various primers showed that the polymerization rate was 50 times slower for all the RNA primers studied, compared to the 18-mer DNA primer (0.2

† B.M.W. and T.R. were supported by a stipend from the German Bundesministerium für Bildung, Wissenschaft, Forschung und Technologie (BMBF; Stipendienprogramm Infektionsforschung).

* Corresponding author. Telephone: 49-231-1206-395. Fax: 49-231-1206-229. Email: tobias.restle@mpi-dortmund.mpg.de.

‡ Max-Planck-Institut für molekulare Physiologie.

§ Present address: Division of Macromolecular Structure, Bristol-Myers Squibb Pharmaceutical Research Institute, Princeton, NJ 08543-4000.

|| Istituto di Strutturistica Chimica.

[1] Abbreviations: HIV-1, human immunodeficiency virus type 1; RT, reverse transcriptase; PBS, primer binding site; dNTP, deoxynucleotide 5′-triphosphate; p/t, primer/template.

S0006-2960(98)01102-7 CCC: $15.00
Published on Web 09/05/1998

s^{-1} and 13 s^{-1}, respectively). Since the RT affinity for the $tRNA^{Lys3}$−p/t initiation complex was found to be comparable to an all-DNA−p/t complex, the low processivity of initiation was attributed to an intrinsically slow incorporation (catalytic step) rate by RT with RNA primer substrates (9). Interestingly, although the rates of polymerization from all of the RNA primers studied were equally slow (of the order of 0.2 s^{-1}), only the natural $tRNA^{Lys3}$ primer efficiently facilitated the transition from the pausing, "initiation" mode, to the fast, processive mode (termed "elongation" mode by the authors; *5*). The more efficient "switch" into the elongation mode was proposed to be due to a more specific interaction between RT with the natural $tRNA^{Lys3}$ annealed to the PBS of the viral RNA template (*5, 9*).

To date, most detailed kinetic characterizations of HIV RT, including binding, catalytic, and drug-resistance mechanisms, as well as structure−function relationships, were carried out using short, p/t substrates in which DNA is the primer. The work presented here characterizes the kinetic and binding parameters for a p/t in which both the primer and template are composed of RNA, thereby addressing the basis of the seemingly slow, nonprocessive activity of transcription initiation. The p/ts studied in this report represent an RNA-only priming ("initiation mode") p/t, a DNA-only priming ("elongation" mode) p/t, and p/ts with primers representing fixed points between initiation and elongation modes (RNA/DNA chimeras). The individual p/t and dNTP binding affinities, in addition to rate constants of polymerization from single-turnover, single dNTP incorporation experiments, reveal the basis of the slow, nonprocessive activity of RT during initiation, as well as the point when (i.e., after how many dNTPs incorporated) the "initiation" p/t turns into an "elongation" p/t. The work further contributes to the notion that initiation is a distinct activity of HIV RT, and therefore a viable target for drug discovery programs.

MATERIALS AND METHODS

Proteins. Recombinant heterodimeric HIV-1 RT was expressed in *E. coli* and purified as described before (10). Enzyme concentrations were routinely determined using an extinction coefficient of 260 450 M^{-1}.

Buffers. All experiments were carried out at 25 °C in a buffer containing 50 mM Tris/HCl, pH 8.0, 10 mM $MgCl_2$, and 20 mM KCl.

Oligonucleotides. Oligodeoxynucleotides were synthesized on an Applied Biosystems 380 B DNA synthesizer. The hybrid oligoribo/oligodeoxynucleotides were synthesized on a Applied Biosystems 392 synthesizer. RNA synthesis was carried out by in vitro transcription with T7 RNA polymerase using synthetic DNA oligonucleotides as described in Milligan et al. (*11*). T7 RNA polymerase was purified according to a protocol described by Jeruzalmi and Steitz (*12*) using the expression system of Studier (*13*). The standard 10 mL T7 reaction mixture contained 40 mM Tris/HCl, pH 8.1, 1 mM spermidine, 0.01% Triton X-100, 50 μg/mL bovine serum albumin (RNase free, Boehringer Mannheim), 8% (w/v) polyethylene glycol 8000, 40 mM dithiohreitol (freshly prepared), 100 mM KCl, 20 mM $MgCl_2$, 4 mM each rNTP (Pharmacia), 1 μM template, and 0.1 mg/mL T7 RNA polymerase. After incubation at 37 °C for 2 h, the reaction was stopped by addition of 50 mM EDTA. The RNA was extracted twice with phenol/chloroform/isoamyl alcohol and precipitated with 1 volume of 2-propanol plus 0.5 M LiCl for 20 min on ice.

All oligonucleotides used in this study were purified by denaturing polyacrylamide gel electrophoresis (15−20% acrylamide, 7 M urea) and eluted from the gel using the Schleicher & Schuell Biotrap unit according to the manufacturer's protocol. Primer and template oligonucleotides were annealed by heating equimolar amounts in 20 mM Tris/HCl, pH 7.5, and 50 mM NaCl for 30 s at 90 °C and then transferred to 70 °C followed by slow-cooling to room temperature in a heat block.

5′-^{32}P-Labeling of Primers. Primers were 5′-end-labeled with T4 polynucleotide kinase (New England Biolabs) using 10 μCi of ^{32}P]ATP (DuPont−New England Nuclear, 3000 Ci/mmol) per 100 pmol of DNA and the reaction buffer supplied from NEB. The reaction was stopped by phenol/chloroform extraction and the primer purified with a ProbeQuant G50 Micro Column (Pharmacia). Concentrations were determined by thin-layer chromatography using a phosphor imager (BioRad) for quantification. Dephosphorylation of the in vitro transcribed RNA primer prior to the end-labeling was carried out according to standard procedures (14).

Fluorescence Measurements of Primer/Template Binding. Affinities of the different p/ts were measured by displacing a fluorescently labeled 18/36-mer DNA/DNA p/t bound to RT (primer sequence, 5′-TCCCTGTTCGGGCGCCAC-3′; template sequence, 5′-TGTGGAAAATCTCATGCAGTG-GCGCCCGAACAGGGA-3′). The fluorescently labeled DNA primer was synthesized by coupling the phosphoroamidite dye 6-FAM, a fluorescein derivative, directly to the 5′-end of the oligodeoxynucleotide during DNA synthesis according to the recommendation of the manufacturer (Applied Biosystems). The titrations were performed using an SLM AB2 spectrofluorometer. To monitor the fluorescence change upon displacing the labeled p/t from RT, the samples were excited at 492 nm, and the emission intensity was measured at 516 nm. These competitive titrations were evaluated by using the program Scientist (MicroMath Scientific Software), which allows the user to define the system under investigation as a series of parallel equations defining (in this case) each discrete equilibrium, the relationship between the total and free concentrations of the components, and the way in which the observable signal is generated. The K_d of the 18/36mer DNA/DNA p/t was determined independently (*15, 16*) and kept constant during the fit procedure.

Rapid Kinetics of Nucleotide Incorporation. Rapid-quench experiments were carried out in a chemical quench-flow apparatus (KinTek Corp., University Park, PA). The apparatus was modified for using small reaction volumes (15 μL). Reactions were started by rapidly mixing the two reactants (15 μL each) and then quenched with 0.6% trifluoroacetic acid (TFA) after defined time intervals. All concentrations reported are final concentrations after mixing in the rapid quench apparatus. Products were analyzed by gel electrophoresis (10% polyacrylamide/7 M urea) and quantitated by scanning the dried gel using a phosphorimager (BioRad). Data were evaluated by the program Grafit (Erithacus Software).

For pre-steady-state kinetics, a preformed complex of p/t−RT (100 nM p/t and 200 nM−3 μM RT, respectively) was rapidly mixed with an excess of dNTP (100 μM−5 mM) and stopped after various times in the millisecond range. Data were fitted to a burst equation (single or double exponential plus a linear equation). The effective pre-steady-state rate constants (k_{pol}) at the given dNTP concentration are derived from the exponential rates.

Affinities of dNTPs were determined by the dependence of the pre-steady-state burst rate on the dNTP concentration. To measure the affinities of the different dNTPs, the p/t−RT complex (100 nM and 200 nM−3 μM, respectively) was rapidly mixed with various concentrations of nucleotide and quenched after $t_{1/2}$ of the maximal pre-steady-state rate (sum of both amplitudes). The corresponding rates were then calculated from the concentration of elongated primer by converting the exponential equation into $k = -\ln[1 - ([P_{+1}]_t/[P]_0)]/t$(s). $[P]_0$ corresponds to the concentration of RT−p/t complex available for incorporation at $t = 0$ (burst amplitude), and t equals the reaction time ($t_{1/2}$ of the maximal pre-steady-state rate). The observed rates were then plotted against the dNTP concentration, and the dissociation constant (K_d) was calculated by fitting the data to a hyperbola. The experiment done in this way measures the K_d for the first step of a two-step dNTP binding mechanism, as shown previously for DNA/DNA p/ts (*16*−*18*) and a DNA/RNA p/t (*17*). The amplitude of the plot of incorporation rate vs concentration of dNTP represents the rate of the second step of nucleotide binding, which is rate-limiting (*19*).

In addition to the fluorescence measurements to determine the affinities of the different p/ts to RT (see above), active site titrations were performed. Here the amount of pre-steady state-nucleotide incorporation as a function of enzyme concentration was analyzed. The data were fitted to a quadratic equation using the program Grafit (*16*). The method of active site titration to determine the affinity of the p/t−RT complexes was chosen since it gave more accurate results for the weakly binding substrates compared to the fluorescence method. The error in using the fluorescence method to calculate the K_d values for the weakly binding substrates is based on the large difference in affinities (2 nM for the fluorescently labeled p/t vs 50 to >200 nM for the hybrid p/ts).

RESULTS

Primer/Template Design. A simplified version of the natural initiation complex was used in this work to avoid ambiguities in the data, such as nonspecific and/or multiple binding sites due to the large size and structural complexity of the natural initiation complex (*8*). This initiation p/t (called PBS_0) is composed of a 20 base RNA primer, containing the 18 base region spanning the primer binding sequence, and a 35 base PBS-containing RNA template (see Figure 1B). The p/t therefore only mimics the initiation complex insofar as the duplex is composed entirely of RNA, and the proper PBS duplex region. In addition to a required 5′-overhang of at least six bases, PBS_0 was constructed to contain a nonpairing end to avoid nonspecific nucleotide incorporation onto a blunt end, a problem observed in our previous work (unpublished observation). The sequence of the template overhang is random, but ensured to contain no

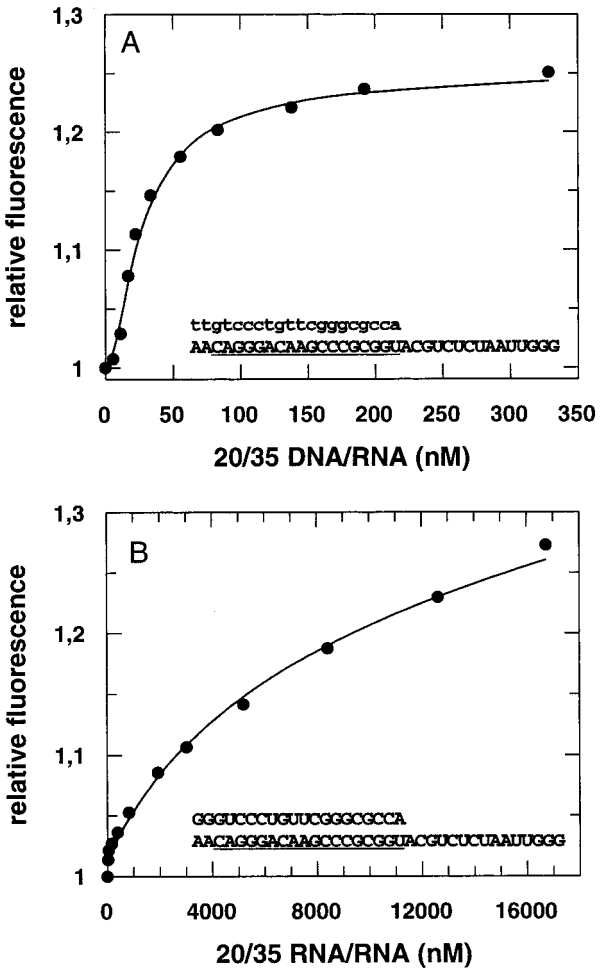

FIGURE 1: Displacement titration of fluorescent p/t bound to RT with PBS_{DNA} (A) and PBS_0 (B) p/ts. A complex of FAM-labeled 18/36-mer DNA/DNA p/t (25 nM) and RT (40 nM) was titrated with increasing amounts of competitor. The curves show the best fit by least-squares fitting to the model describing the two binding equilibria from which dissociation constants of 1 nM (±0.9) for PBS_{DNA} and >200 nM for PBS_0 were obtained (see Materials and Methods). The insets show the sequence of the two p/ts used for displacement. The primer binding region is underlined. RNA is shown in upper case letters, and DNA is given in lower case letters. The sequence of the DNA/DNA p/t is shown in Table 1.

defined secondary structure, as determined by using the RNA secondary structure prediction program RNA fold in PC/Gene, based on the Zuker method (*20*). An "elongation" p/t was studied for comparison (called PBS_{DNA}; see Figure 1A), which contains a DNA primer.

Affinity of RT for the RNA/RNA p/t Compared to the DNA/RNA p/t. To compare the single-turnover nucleotide incorporation kinetics for an initiation (RNA) vs an elongation (DNA) primer, it was important to measure the binding affinities for these p/ts and for the next, correct dNTP to be incorporated (dTTP). This is to ensure that the single-turnover rate of incorporation observed is limited by internal rate-limiting kinetic parameters, rather than by binding parameters, which occurs when concentrations are used below the saturation level. The p/t affinities were measured by a displacement titration using a fluorescently labeled DNA/DNA p/t, for which the affinity is already known (*15*). RT is precomplexed to the fluorescent p/t, and then displaced by increasing amounts of one of the PBS p/ts. The fluorescence increase observed upon displacement of the

fluorescent p/t into solution is measured, as shown in Figure 1. The K_d is derived from a least-squares fit of the data to a model describing both equilibria (see Materials and Methods). For PBS_{DNA}, the fit yielded a K_d of 1 nM (Figure 1A), in agreement with the K_d previously measured for a 25-mer DNA primer/45-mer RNA template substrate (~5 nM; *17*). For PBS_0, the binding was observed to be weak and almost unmeasurable. The fit to the data shown in Figure 1B, yielding a K_d of >200 nM, contains a large error, presumably introduced by the large difference in affinity compared to the fluorescently labeled p/t. The K_d value is therefore assigned to a range of 200−1000 nM. The results indicate that micromolar amounts (≥3 μM) of RT must be used in the single-turnover experiments in order to achieve saturation binding of the 100 nM PBS_0 used in the studies (see below).

Deoxynucleotide Binding Affinity and Incorporation Rate for the RNA Primer Compared to the DNA Primer p/t Substrates. The binding constants of the incoming nucleotide (dTTP) for the RT-bound p/ts PBS_0 and PBS_{DNA} were measured to ensure that saturating concentrations of nucleotide are used during the single-turnover experiments described later in this work. The dissociation constants were derived by measuring the dTTP concentration dependence of the single-turnover rate of product formation (extending the 20-mer primer to a 21-mer), as described for previous studies (*16*−*18*). The experiments therefore determined not only dTTP K_ds but also the maximal, single-turnover incorporation rate (amplitude of the fits to the plots in Figure 2; see Materials and Methods). The plot of the rate of single dTTP incorporation into PBS_0 or PBS_{DNA} vs the concentration of dTTP is shown in Figure 2. The best fit to the hyperbolic equation relating the rate of incorporation to the concentration of dTTP yielded a dTTP dissociation constant (K_d) of 6.6 μM for the PBS_{DNA} p/t (Figure 2A), consistent with previous measurements of dNTP affinities using DNA primers (5−10 μM; *16*−*19*, *21*). Although both sets have identical sequences and incorporate the same dNTP, the affinity of the dNTP for PBS_0 (K_d ~ 3.4 mM) was found to be at least 500 times lower than that of the DNA/RNA p/t, PBS_{DNA}. The data also show that at saturating amounts of RT and dTTP, the incorporation rate for PBS_0 is about 50 times slower than the PBS_{DNA} rate (0.78 s^{-1} and 35 s^{-1}, respectively), consistent with the difference in rates observed for more natural initiation compared to elongation complexes observed by Lanchy et al. (*9*).

Deoxynucleotide Binding Affinity for a DNA Primer Preextended by One Ribonucleotide. The data in Figure 2 show that the binding of a dNTP to an RT-bound p/t containing an RNA primer is very weak compared to that of a DNA primer. The lower affinity could be due to the presence of a ribonucleotide (2′-hydroxyl group) instead of a deoxynucleotide (2′-hydrogen) at the 3′-end of the PBS_0. In addition, the lower affinity for PBS_0 could result from a different RT-bound orientation, and thus altered dNTP binding pocket of the duplex RNA p/t compared to the DNA/RNA duplex. To test this, a DNA primer preextended by one ribonucleotide (called $PBS_{DNA+1RNA}$; see Table 1) was characterized. The affinity of this p/t for RT was measured as before, yielding a dissociation constant of 3 nM, indistinguishable from that of the unextended PBS_{DNA} (data not shown). Measurement of the affinity for the next incoming

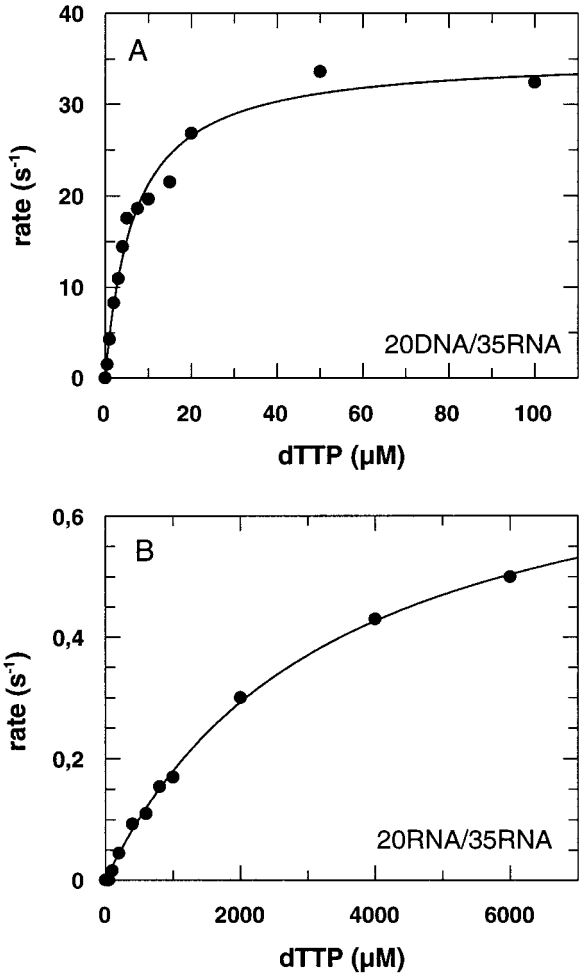

FIGURE 2: Dependence of the pre-steady-state burst rate on dTTP concentration. Increasing amounts of dTTP were rapidly mixed with a preincubated solution of RT and p/t. Final concentrations after mixing were 200 nM RT, 100 nM PBS_{DNA} (A); and 3 μM RT, 100 nM PBS_0 (B). The curves show the best fit of the data to the hyperbolic equation relating the rate of incorporation to the concentration of dTTP (see Materials and Methods), yielding dTTP K_d values of 6.6 μM (±0.7) for PBS_{DNA} and 3.4 mM (±0.2) for PBS_0.

nucleotide, dGTP, yielded a dissociation constant of 5 μM, also in the range of that measured for nucleotide binding to PBS_{DNA} (and consistent with previous measurements of the K_d of dGTP for other DNA p/ts; *22*). The dramatically lower affinity of dTTP for PBS_0 is therefore due to other factors than the presence of a ribonucleotide on the 3′-end. Interestingly, the single-turnover rate of incorporation for $PBS_{DNA+1RNA}$ (k_{pol} ~ 3.7 s^{-1}) is faster than PBS_0 (~0.78 s^{-1}), but an order of magnitude slower than that of PBS_{DNA}. Although the $PBS_{DNA+1RNA}$ p/t and dNTP are bound tightly, the slower rate of incorporation suggests that orientation of the terminal ribonucleotide is suboptimal, or that the 2′-OH group somehow interferes with the catalytic mechanism.

Single-Turnover Nucleotide Incorporation Time Courses for the RNA/RNA Compared to the DNA/RNA p/t Substrates. The single-turnover kinetics of dTTP incorporation appeared to be slower for PBS_0 compared to PBS_{DNA} (Figure 2). The time courses of dTTP incorporation for PBS_0 and PBS_{DNA}, using saturating amounts of enzyme and dTTP, are shown in Figure 3. Previous characterizations of a variety of DNA/DNA and of DNA/RNA p/ts, using p/t concentrations in

Table 1: Summary of the Parameters for p/t and dNTP Binding and dNTP Incorporation

primer/templates [a]		K_d p/t (nM)	K_d dNTP (μM)	rates (s^{-1}) k_{pol1} and k_{pol2} [b]
GGGUCCCUGUUCGGGCGCCAt AACAGGGACAAGCCCGCGGUACGUCUCUAAUUGGG	PBS_0	> 200	3400 (± 200)	8.5 (± 1.7), 0.5 (± 0.07)
GGGUCCCUGUUCGGGCGCCAtg AACAGGGACAAGCCCGCGGUACGUCUCUAAUUGGG	PBS_{+1}	> 200	305 (± 42)	0.9 (± 0.04) [c]
GGGUCCCUGUUCGGGCGCCAtgca AACAGGGACAAGCCCGCGGUACGUCUCUAAUUGGG	PBS_{+3}	213 (± 22)	2.4 (± 0.2)	23 (± 6.5), 0.35 (± 0.04)
GGGUCCCUGUUCGGGCGCCAtgcaga AACAGGGACAAGCCCGCGGUACGUCUCUAAUUGGG	PBS_{+5}	92 (± 9.6)	24 (± 3.2)	21 (± 4.9), 0.8 (± 0.1)
GGGUCCCUGUUCGGGCGCCAtgcagag AACAGGGACAAGCCCGCGGUACGUCUCUAAUUGGG	PBS_{+6}	42 (± 2.7)	36 (± 3.2)	23 (± 2.4), 0.6 (± 0.2)
GGGUCCCUGUUCGGGCGCCAtgcagaga AACAGGGACAAGCCCGCGGUACGUCUCUAAUUGGG	PBS_{+7}	9 (± 1.1)	67 (± 3.7)	19 (± 1), 1.3 (± 0.4)
GGGUCCCUGUUCGGGCGCCAtgcagagat AACAGGGACAAGCCCGCGGUACGUCUCUAAUUGGG	PBS_{+8}	6 (± 1)	41 (± 1.2)	19 (± 3.2), 1.9 (± 0.7)
ttgtccctgttcgggcgccat AACAGGGACAAGCCCGCGGUACGUCUCUAAUUGGG	PBS_{DNA}	1 (± 0.9)	6.6 (± 0.7)	52 (± 6.4), 5 (± 5)
ttgtccctgttcgggcgccaUg AACAGGGACAAGCCCGCGGUACGUCUCUAAUUGGG	$PBS_{DNA+1RNA}$	3 (± 0.8)	5 (± 0.2)	3.7 (± 0.17) [c]
tccctgttcgggcgccact agggacaagcccgcggtgacgtactctaaaaggtgt	DNA/DNA	2 (± 0.2)	9.2 (± 0.2)	82 (± 25), 1.4 (± 0.2)

[a] RNA is shown in upper case letters, and DNA is given in lower case letters; the boldface letters represent the nucleotides to be incorporated. [b] The two exponential phases represent the single-turnover dNTP incorporation kinetics of two different RT-bound forms of the p/t: a fast, kinetically competent bound form, incorporating a dNTP at a rate of 10−50 s^{-1} (k_{pol1}); and a slow, less-competent bound form, incorporating at a rate of 0.3−1 s^{-1} (k_{pol2}). [c] PBS_{+1} and $PBS_{DNA+1RNA}$ were fitted to a single-exponential equation plus slope.

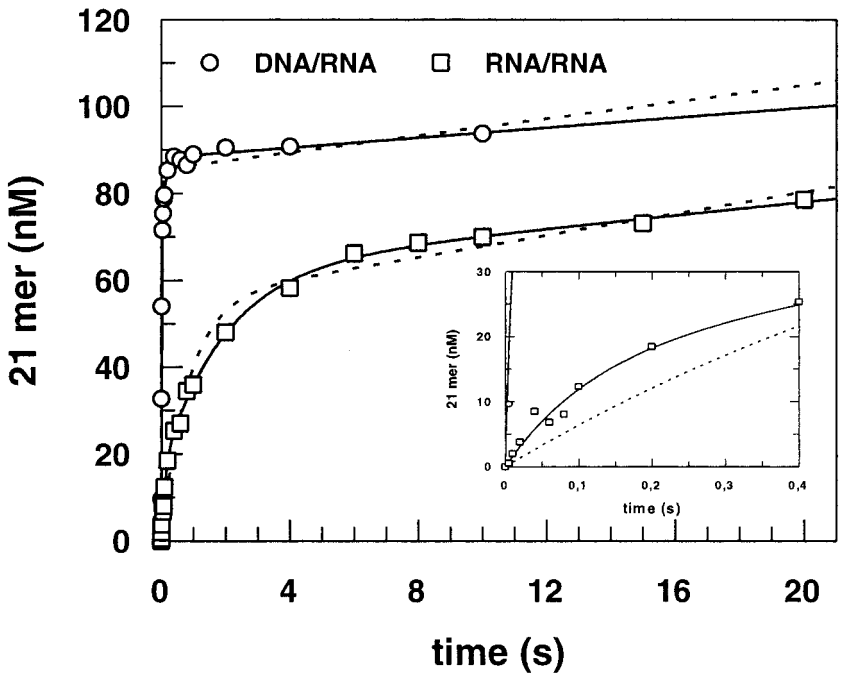

FIGURE 3: Comparison of the single-turnover, single-dTTP incorporation into PBS_0 and PBS_{DNA}. Data were fitted to a double-exponential equation plus slope (boldface lines) or to a single-exponential equation plus slope (dashed lines). (○) A preformed complex of 100 nM PBS_{DNA} p/t and 200 nM RT was mixed with 100 μM dTTP. In the case of PBS_0 (□), 100 nM p/t and 3 μM RT were mixed with 5 mM dTTP. The double-exponential analysis of the experimental data yielded burst rates (k_{pol1} and k_{pol2}) of 8.5 s^{-1} (±1.7) and 0.5 s^{-1} (±0.07) for PBS_0, and 52.5 s^{-1} (±6.3) and 5.5 s^{-1} (±5) for PBS_{DNA}. The single-exponential analysis gave a burst rate (k_{pol}) of 0.5 s^{-1} (±0.05) for PBS_0 and 43 s^{-1} (±3.3) for PBS_{DNA}. Comparison of the reduced χ^2 values for single- vs double-exponential analysis for PBS_0 and PBS_{DNA} gave values of 13.4 and 12.3 vs 1.8 and 8.6, respectively. The inset shows the reaction on a shorter time scale.

excess over RT, showed that the dNTP is incorporated with a single-exponential burst of product formation (single-turnover rate) followed by a slower linear phase. The linear, steady-state phase was shown to be caused by the rate-

limiting dissociation of the extended p/t product, which must occur before more p/t can be turned over (*17*). Both time courses in Figure 3 contain a burst and a linear phase. Since the concentration of RT used in both experiments was in excess over p/t, a linear phase was not expected. Furthermore, the burst amplitude, especially for PBS_0, is clearly lower than 100 nM. Although RT should be saturated with p/t (concentrations are considerably higher than K_ds), a portion of the p/t appears to bind nonproductively. This effect is examined in detail in a later section.

Initial fitting of the data in Figure 3 was carried out using an equation including the sum of a single-exponential and a linear equation. The single-turnover rates were thereby determined to be $\sim$43 s^{-1} for PBS_{DNA} and $\sim$0.5 s^{-1} for PBS_0, consistent with those found from the amplitudes of the plots shown in Figure 2. The data, especially for PBS_0, however, appear to deviate from a single exponential in the first 0.6 s of turnover, as illustrated in the inset plot in Figure 3. The data clearly fit better to the sum of two exponentials (solid lines in Figure 3), plus the linear contribution. The observation was found to be reproducible, and is further examined in the next sections.

Binding Parameters for p/ts with RNA Primers Preextended with Increasing Numbers of Deoxynucleotides. Both the p/t and the dNTP binding affinities varied significantly between the all-RNA primer, "initiation-p/t" PBS_0, and the all-DNA primer, "elongation-p/t" PBS_{DNA}. To determine how many dNTPs added on the RNA primer substrate transform the p/t functionally into a DNA primer-like substrate, the nucleotide and p/t binding constants were measured for p/ts consisting of the PBS_0 extended with one, three, five, six, seven, or eight dNTPs (see Table 1 for structures and nomenclature). Table 1 summarizes the results.

The dissociation constants for the various p/ts were measured by fluorescence displacement titrations, as described earlier, and by active site titrations, analyzing the dependence of the amount of pre-steady-state nucleotide incorporation on the RT concentration (see Materials and Methods). The method of active site titration to determine the p/t affinity was found to yield more accurate results for the weakly binding substrates, compared to the fluorescence method. As described for the PBS_0 K_d determination, the fluorescence method yields large errors in the fits, introduced from the large difference in affinity of the p/ts compared to the fluorescently labeled p/t (K_ds 50 to >200 nM for the hybrid p/ts, and $\sim$2 nM for the labeled p/t). The results of the K_d determinations are summarized in Table 1. As the number of deoxynucleotides present on the 3′-end of the RNA primer increases, the affinity of RT for the p/t increases, from the lowest affinity with no deoxynucleotides (PBS_0, K_d > 200 nM) to the highest affinity with all deoxynucleotides (PBS_{DNA}, $K_d \sim 1$ nM). The binding appears to be weak and essentially nonspecific (K_ds $\geq$ 200 nM) for the p/ts containing zero to three deoxynucleotides. After that, the affinity increases incrementally with each deoxynucleotide addition, until eight (PBS_{+8}) when the affinity is almost comparable to that of the all-DNA primer p/t, PBS_{DNA}. Among the higher affinity hybrid p/ts (PBS_{+6}, PBS_{+7}, and PBS_{+8}), good agreement was found between the fluorescence and active site titration methods (data not shown).

Deoxynucleotide binding affinities were measured as described for PBS_0 and PBS_{DNA}. Table 1 summarizes the results, and shows that the pattern essentially follows an increasing affinity with increasing number of deoxynucleotides present on the 3′-end of the primer. The largest enhancement of dNTP affinity compared to PBS_0 appears to be for the p/t extended by one and three deoxynucleotides, which increases the dNTP affinity by at least an order of magnitude for each extented p/t ($K_d(PBS_0) \sim 3.4$ mM; $K_d(PBS_{+1}) \sim 305$ μM; $K_d(PBS_{+3}) \sim 2.4$ μM). The affinity of dATP with PBS_{+3}, $K_d \sim 2.4$ μM, was reproducibly measured to be higher than the nucleotide affinities measured using all the p/ts in this study. The affinity is also higher than that of dATP for an all-DNA p/t (*17*). The reason for this higher affinity is unknown. From PBS_{+5} to PBS_{+8}, the affinities for dNTPs (K_ds 24−41 μM) appear to be fairly constant and almost an order of magnitude lower than the all-DNA primer, PBS_{DNA} ($K_d \sim 6.6$ μM). As before, these affinity measurements allowed determination of substrate and RT concentrations to be used in the comparative single-turnover experiments described in the next section.

Single-Turnover Nucleotide Incorporation Kinetics for p/ts with RNA Primers Preextended with Increasing Numbers of Deoxynucleotides. The single-turnover incorporation time courses for the various preextended RNA primer p/ts, with the exception of PBS_{+1} and $PBS_{DNA+1RNA}$, displayed a significant and reproducible deviation from the single-exponential plus linear profile previously reported for p/t incorporation kinetics (*16*−*18*, *21*, *23*). The effect was also observed for PBS_0, as described earlier (see Figure 3). Figure 4 illustrates with the PBS_{+3} and PBS_{+5} p/ts how the time courses of dNTP incorporation clearly showed a burst of product formation, followed by a second, slower exponential phase, followed by a linear phase. The expanded plot in Figure 4B shows the difference between fitting the data to a single-exponential equation (plus linear equation) compared to an equation including the sum of two exponentials (plus linear equation). The points in the first $\sim$0.3 s of turnover are clearly missed by the single-exponential fits.

Fitting of the time courses for all of the preextended RNA primer p/ts, in addition to those for PBS_0 and PBS_{DNA}, to a biexponential plus linear equation yielded similar rates for the first, fast exponential phase ($\sim$10−50 s^{-1}) and for the second exponential phase ($\sim$0.3−1 s^{-1}; results are summarized in Table 1). Since the concentrations of RT and dNTP used in the experiments are saturating, the two exponential phases represent the single-turnover dNTP incorporation kinetics of two different RT-bound forms of the p/t: a fast, kinetically competent bound form, incorporating a dNTP at a rate of 10−50 s^{-1} (k_{pol1}); and a slow, less-competent bound form, incorporating at a rate of 0.3−1 s^{-1} (k_{pol2}).

The observation of two exponentials in the time course of dNTP incorporation extends to the all-DNA primer p/t, PBS_{DNA}, as well as to the DNA/DNA p/t (data not shown), which is the p/t analogous to most p/ts characterized to date. Although the data in Figure 3 for PBS_{DNA} appear to fit well to a single-exponential (plus linear) equation, closer examination found that a double exponential fits the data more precisely. Since the amplitude of the second phase is small relative to the amplitude defining the first, fast phase, the fit

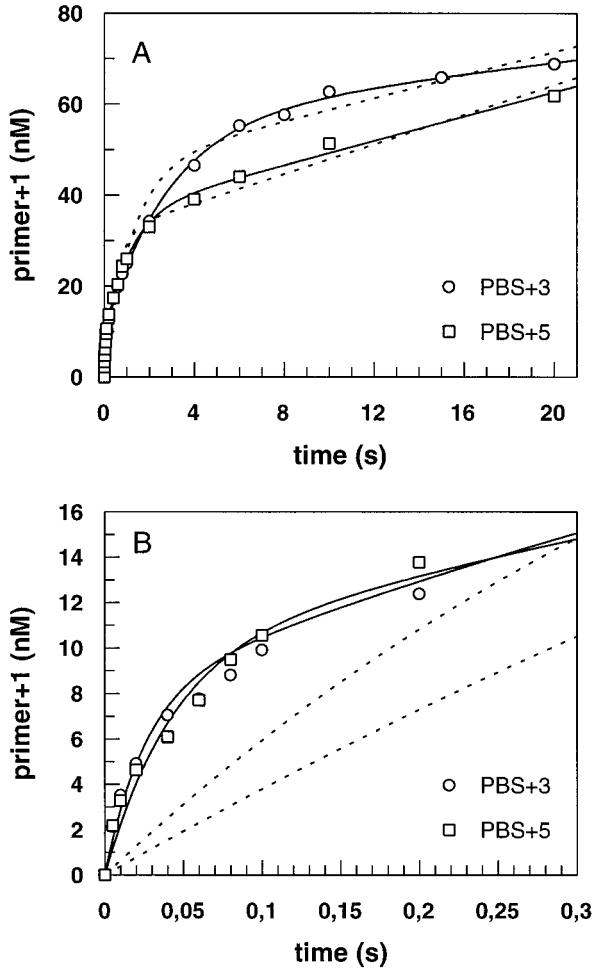

FIGURE 4: Single-turnover kinetics of the incorporation of dATP into PBS_{+3} and PBS_{+5}. A preformed complex of 100 nM PBS_{+3} p/t and 1 μM RT was mixed with 1 mM dATP (○). In the case of PBS_{+5} (□), 100 nM p/t and 1 μM RT were mixed with 500 μM dATP (A). The analysis of the experimental data using a double-exponential equation plus slope yielded k_{pol1} and k_{pol2} rates of 23 s^{-1} (±6.5) and 0.3 s^{-1} (±0.04) for PBS_{+3} and 21 s^{-1} (±4.9) and 0.7 s^{-1} (±0.09) for PBS_{+5}, respectively. The dashed curves represent the best fits to a single-exponential equation plus slope. A comparison of the reduced χ^2 values for single- vs double-exponential analysis for the PBS_{+3} and PBS_{+5} data gave numbers of 16 and 11 versus 1.3 and 0.9, respectively. (B) shows the reaction on a smaller time scale.

of the data to a single-exponential (plus linear) equation yields a rate (43 s^{-1}) close to the rate of the first exponential (52 s^{-1}) from a fit to the double-exponential equation. Analysis of a DNA/DNA p/t also found that the data similarly fit best to a double-exponential equation plus slope (data not shown; T.R. and B.M.W., manuscript in preparation).

Comparison of the Single-Turnover Time Courses of All Primer/Templates. All of the p/ts listed in Table 1 (except PBS_{+1} and $PBS_{DNA+1RNA}$) have similar rates (k_{pol1} and k_{pol2}) corresponding to the two productive RT-bound forms. But the respective time courses varied dramatically, going from the overall slow time course shown for PBS_0 to the overall fast time course seen for PBS_{DNA} (see Figure 3). Since the different p/ts varied in the amount of total (100 nM) p/t that binds productively (discussed in the next section), comparison of all p/ts in one plot was found to be best accomplished by normalizing the data. Figure 5 shows the time courses plotted after normalization, where 100% equals the total

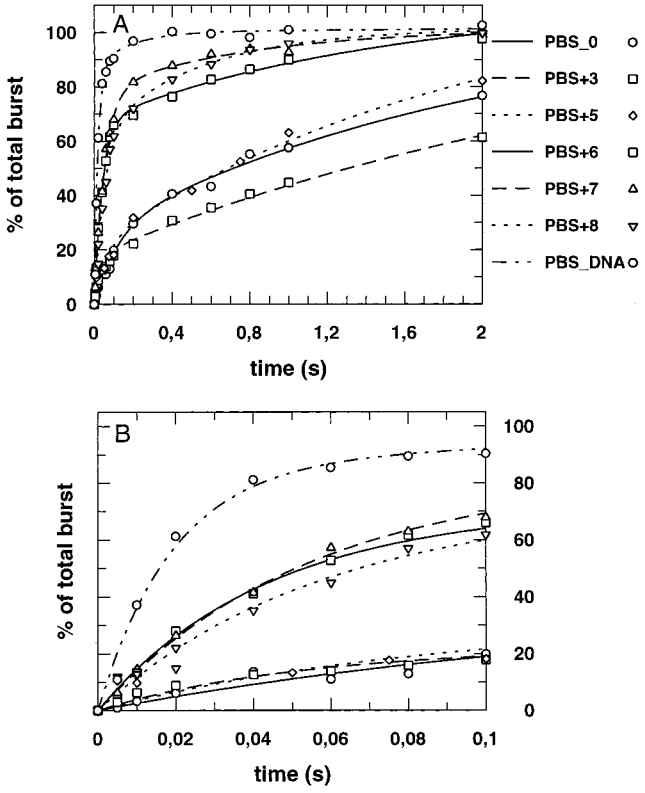

FIGURE 5: Summary of the single-turnover, single-nucleotide incorporation time course for the different p/ts used in this study. All data were fitted to a double-exponential equation plus a slope. The data were normalized so that 100% incorporation equals the sum of the two burst amplitudes. The curves for PBS_{+1} and $PBS_{DNA+1RNA}$ are not shown. (A) Time courses showing both exponential phases; and (B) expansion of the first 0.12 s of the time courses in (A), to illustrate the percentage incorporated in the fast first phase. A summary of the observed burst rates and the relative distribution of the burst amplitudes is given in Table 1 and Figure 6, respectively.

amount of p/t bound productively (i.e., the sum of the two exponential amplitudes).

The difference between the p/t time courses lies in the relative amplitudes of the two exponential phases. Figure 5 shows that with an increasing number of deoxynucleotides located on the 3′-end of the primer, the amplitude of the first fast phase increases, while that of the slow phase decreases. For PBS_0, PBS_{+3}, and PBS_{+5}, most of the single-turnover time course (~80%) is represented by the slow, $k_{pol2} \sim 0.3-0.5$ s^{-1}, p/t-bound form, while only ~20% of the p/t is bound in the fast form, $k_{pol1} \sim 9-23$ s^{-1}. Starting from six deoxynucleotides located on the 3′-end of the primer, PBS_{+6}, the distribution switches: more (> 60%) of the p/t is bound in the fast, kinetically competent form than in the slow form. The switch to an overall more kinetically competent p/t substrate after six deoxynucleotides are incorporated is best illustrated by Figure 5B and Figure 6. Figure 5B shows the portion of the time courses in Figure 5A that are completely due to the fast, kinetically competent form of the bound p/t (first exponential). A jump in the size of the amplitude of the first exponential phase, when going from PBS_{+5} to PBS_{+6}, can be clearly seen. For PBS_{+5}, the fast phase correlates to ~20% of the bound p/t, while for PBS_{+6}, the fast phase correlates to greater than 60% of the bound p/t. PBS_{DNA} represents the optimal substrate with almost all (~90%) of the p/t bound in the fast form. The

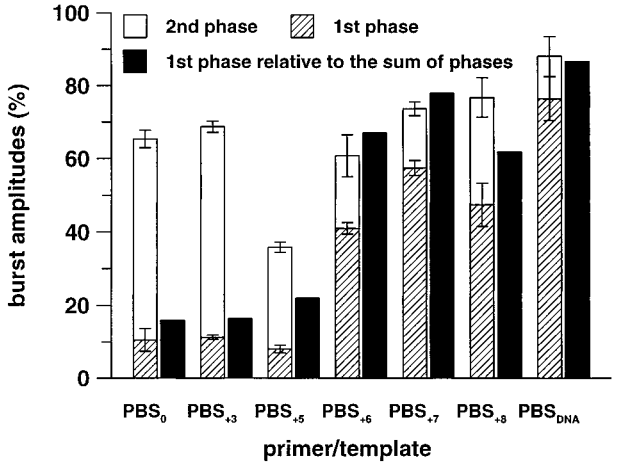

FIGURE 6: Graphical representation of the distribution of the two burst amplitudes for single-turnover nucleotide incorporation for the different p/ts. The overlapping open and hatched columns show the percentage of the two burst amplitudes relative to the maximal possible incorporation of dNTP as calculated by the double-exponential fit (see Figure 5). The first amplitude (representing the fast phase, ~10−50 s^{-1}) is given by the hatched area, and the second amplitude (representing the slow phase, ~0.3−1 s^{-1}) is given by the open area. The black columns represent the percentage of the first amplitude relative to the sum of the amplitudes. The errors are indicated by error bars.

amplitudes of the fast phase from the time courses in Figure 5 are replotted as black-filled columns in the summary plot shown in Figure 6.

Productive and Nonproductive Primer/Template Binding. The concentration of p/t used in all of the kinetic experiments was 100 nM. Although the affinity measurements determined that all (100 nM) of the p/t should bind to the RT present (in excess), the total amount of the p/t bound in a productive manner (sum of the fast and slow burst sizes) was consistently observed to be less than 100 nM. The percent of the 100 nM p/t used in the experiments that is RT-bound and extended by one dNTP (productive fast and slow forms) is depicted by the overlapping open and hatched columns in Figure 6. The hatched columns represent the percent of total 100 nM p/t that binds and incorporates dNTP with the fast (k_{pol1} ~ 10−50 s^{-1}) polymerization rate, while the open column represents the rest of the productively bound p/t that incorporates at the slower (k_{pol2} ~ 0.3−1 s^{-1}) polymerization rate. For PBS_0, the total amount of p/t bound productively is ~65 nM (65%), with ~10 nM (10%) bound in the fast form, and 55 nM (55%) in the slow form. The rest of the p/t (35 nM or 35%) binds to RT nonproductively. For PBS_{DNA}, for which the affinity is more precisely known (K_d ~ 1 nM), 100% of the 100 nM p/t must be bound to the 200 nM RT used in the experiment, and yet ~88% (88 nM) of the bound p/t is bound productively, with ~75 nM bound in the fast form, and ~10 nM in the slow form. Twelve nanomolar, or 12%, is therefore bound nonproductively.

The linear phase of product formation, following the two burst phases, corresponds to turnover of the rest of the p/t used in the experiment. To test whether the linear phase represents the nonproductive binding fraction of p/t, and therefore corresponds to the rate-limiting dissociation of nonproductively bound p/t (that must dissociate and rebind productively to be turned over), the single-turnover experiment (using 100 nM DNA/DNA or DNA/RNA p/ts and 200 nM RT) was carried out in the presence of an excess amount of competing p/t [2 μM poly(rA)/oligo(dT)] as a trap. The resulting time course showed a total burst size (amplitude) equal to that of the time course carried out in the absence of trap, but no longer contained a linear phase (data not shown; T.R. and B.M.W., manuscript in preparation). The linear phase in the time courses therefore corresponds to the fraction of p/t bound nonproductively, and incorporation occurs only after the p/t dissociates (rate-limiting) and rebinds as one of the productive complexes.

The plot in Figure 6 shows that the amount of nonproductively bound p/t decreases slightly with increasing number of deoxynucleotide incorporations. PBS_{+5} was the exception, and reproducibly showed a majority of nonproductively bound fractions (~60%). The DNA/DNA p/t (data not shown) kinetics also displayed a high amount of p/t bound nonproductively (~50% or 50 nM of the 100 nM), consistent with reports from previous studies with similar p/ts, which found burst sizes of the order of 50% of the total p/t used in the experiment (*17*). The results therefore define three modes of p/t binding to RT, the relative amounts of each depending on how many deoxynucleotides comprise the 3′-end of the primer: a fast, kinetically competent form (single-turnover rate ~10−50 s^{-1}); a slow form (single-turnover rate ~0.3−1 s^{-1}); and a dead-end form (no turnover).

DISCUSSION

The goal of this work was to determine the basis of the slow, nonprocessive polymerization reaction catalyzed by RT during transcriptional initiation, when both the primer and template are composed of RNA. The studies examined whether the slower activity, compared to DNA-primed transcription, is merely a binding effect, or whether incorporation of a deoxynucleotide onto the 3′-end of RNA is inherently inefficient or slow (a catalytic effect), as suggested by the work of Ehresmann and co-workers (9), using more natural p/t species. The results were also anticipated to reveal when, i.e., after how many dNTPs incorporated, the "initiation" p/t turns functionally into the optimal, processive "elongation" p/t.

The results presented show that RT binds the RNA/RNA duplex PBS_0 very weakly and nonspecifically compared to the corresponding DNA primer p/t substrate, PBS_{DNA}. A weaker binding affinity was also measured for the p/t complex formed from a synthetic form of $tRNA^{Lys3}$ compared to an 18-mer DNA oligonucleotide annealed to a 300 base RNA template (*9*). At saturating enzyme concentration, the binding affinity of the incoming deoxynucleotide, dTTP, to the RT−PBS_0 complex (K_d ~ 3.4 mM) is dramatically lower than the dNTP affinity using PBS_{DNA} (K_d ~ 6.6 μM), or any other DNA primer containing p/t reported in the literature (*16*−*19*, *21*−*25*). The pausing, nonprocessive activity during initiation is therefore at least in part due to the lower p/t and dNTP affinities for an RNA/RNA duplex.

Initial analysis of the single-turnover time courses for the incorporation of single dNTPs into RNA and DNA primer p/t substrates showed that the overall rate of incorporation for PBS_0 is about 50 times slower than the PBS_{DNA} rate (0.78 s^{-1} and 35 s^{-1}, respectively). This apparently slower catalytic rate for RNA-primed polymerization is consistent with the results reported by Lanchy et al. (9), who also found

a 50-fold difference in the dNTP incorporation rates for an oligodeoxynucleotide-primed (13 s^{-1}) vs oligoribonucleotide-primed (0.2 s^{-1}) reaction. The experiments reported by these authors, however, measured the incorporation rate of two nucleotides, at concentrations of only 50 μM each. If the dissociation constants of the dNTP for the RNA-priming initiation complexes used in their studies are also in the millimolar range, the rates of incorporation measured may not be maximal.

Further analysis revealed that the slower polymerization rate during initiation is not due to a single, slow incorporation mode. Comparison of the pre-steady-state time courses for PBS_0, for PBS_{DNA}, and for p/ts containing RNA primers preextended by increasing numbers of dNTPs showed that, with the exception of PBS_{+1} and $PBS_{DNA+1RNA}$, single dNTP incorporation occurs in two exponential phases (two bursts), followed by a linear phase. Each exponential was found to represent a different mode of productive p/t binding, a fast mode and a slow mode, where fast and slow refers to the catalytic efficiency. The linear phase was found to be due to a fraction of the p/t bound in a nonproductive manner. While the overall slower polymerization during initiation is due to a large portion of the p/t bound in a slow form (second exponential burst phase in the time course), some of the p/t is bound in a kinetically competent mode (first exponential burst phase), incorporating nucleotide with a rate comparable to that of DNA-primed transcription.

At least three different p/t−RT binding modes therefore exist when p/t is incubated with RT, and the relative amounts of each mode depend on how many deoxynucleotides comprise the 3′-end of the RNA primer. It is unclear why PBS_{+1} and $PBS_{DNA+1RNA}$ reproducibly exhibited a single, slow mode of incorporation. The first, fast-reacting p/t binding mode represents the optimal binding mode for p/t, resulting in an incorporation rate in the maximal range ($k_{pol1} \sim 10-50$ s^{-1}) observed for HIV RT using a variety of DNA-priming p/ts (*16*−*18*, *21*, *23*). The second, slow form also represents a productive binding mode, but incorporates ($k_{pol2} \sim 0.3-1$ s^{-1}) the incoming nucleotide at least an order of magnitude more slowly than the fast form. The third type of binding mode is the nonproductive, dead end form, with no turnover possible. The trap experiment demonstrated that in order to incorporate a dNTP, the nonproductively bound p/t must dissociate and rebind in one of the productive forms.

The different K_ds for dNTP and p/t found for the various p/ts, in combination with the varying distribution of binding modes depending on the number of deoxynucleotides incorporated, suggest that the two productive p/t binding modes have correspondingly different dNTP and p/t affinities. As the fraction of p/t bound in the fast, kinetically competent form increases, the affinities of the p/t and dNTP generally increase too. This means that the affinities determined in this work reflect *overall* affinities, representing an average of a mixture of different binding species. Since the majority of the p/t is bound to RT in one of the two possible productive modes (except for PBS_{+5}; see Figure 6), the K_d determinations (by active site titrations) are therefore most representative of the predominantly bound form. In other words, the K_ds of RT−PBS_0 for dTTP and p/t were measured from the turnover corresponding to the majority bound species (∼84%), which is the slow form. The small percentage of PBS_0 (∼16%) bound in the fast, kinetically competent form presumably contributes a relatively insignificant amount to the K_d measurement.

Since the nucleotide binds to the RT−p/t complex, and not to RT alone (*19*, *26*), the p/t is involved in creating a binding site for the nucleotide (*27*). Most of the DNA primer p/t, PBS_{DNA}, is bound in the fast form, for which both the binding affinities and polymerization rate are maximal. The fast form therefore represents the optimal orientation of the p/t for creation of an optimal binding site for the nucleotide. For PBS_0, whose predominant binding mode is that of the slow productive form, the nucleotide binding affinity is dramatically lower than that of PBS_{DNA}. But characterization of a p/t consisting of a DNA primer extended with one ribonucleotide revealed a normal nucleotide binding affinity ($K_d \sim 5$ μM), comparable to that of DNA primer p/ts. The lower dTTP binding affinity for PBS_0 compared to PBS_{DNA} is therefore not due to the presence of the 2′-hydroxyl group on the terminal nucleotide of the RNA primer. For PBS_{+3} and PBS_{+5}, however, whose predominant binding mode is also that of the slow form, nucleotide binding is close to optimum (K_ds $\sim$ 2.4 μM and 24 μM, respectively). These results suggest that, with exception to PBS_0, the slow productive form represents a mode of p/t binding that orients the dNTP properly for the first step of binding (resulting in normal dNTP affinities), but improperly or suboptimally for triggering the rate-limiting, second step of nucleotide binding, which is thought to be rate-limiting for the incorporation. For RT, and other polymerases, this rate-limiting step has been proposed to involve a closing of the "fingers" domain, during the second step of nucleotide binding (for a review, see *27*).

Characterization of the preextended RNA primer p/ts showed that once six dNTPs are incorporated, a majority of the resulting p/t binds to RT in the fast kinetically competent form. The definition of the "switch" from initiation to elongation can therefore be defined as the point when more of the p/t binds in the fast, productive mode than in the slow productive, or nonproductive mode. The structural basis for this switch remains to be addressed. Also unknown is the basis of the low affinity of dTTP for PBS_0, compared to other p/ts that also bind predominantly in the slow mode. Insights may come from comparison of the structural features of the p/t-bound form of RT and of other polymerases (for a review, see *27*, *28*). The crystal structure of RT complexed to a p/t showed that the 18/19-mer duplex DNA assumes an A-like form in the first 5−7 bases of the duplex, followed by a 40−45° bend in the DNA, as the rest of the duplex assumes the B form, which extends from the polymerase active site into the RNase H active site (*29*). Furthermore, recent structural analysis of a p/t-bound form of T7 DNA polymerase also showed an A to B form transition, occurring after two bases from the 3′-terminus of the primer, and for the structure of *Bacillus stearothermophilus* DNA polymerase, the transition occurs between the fourth and fifth base (*30*, *31*). Both structures showed that the A to B transition represents a transition from C3′-endo to C2′-endo sugar puckering. The conformation of the A-like form of the 3′-terminal region of the primer, with C3′-endo sugar puckering, creates a widening of the minor groove, presumably providing the necessary access of protein side chains to nucleotide bases (*32*, *33*).

The significance of the A to B transition is that it can occur only for DNA/DNA or RNA/DNA hybrids (*34*). Both the crystal and solution structures of an RNA/DNA duplex hybrid showed that the conformation assumes neither an A nor a B form (*35*−*37*). While the sugars of the RNA strand adopt the C3′-endo conformation, the DNA strand adopts an intermediate, O4′-endo conformation which results in a narrowing of the minor groove. This intermediate conformation of the sugars is impossible for an RNA/RNA duplex to adopt, due to the 2′-hydroxyl groups which lock the RNA in the A form (*34*). The all-RNA duplex PBS_0 p/t cannot adopt the A to B transition which appears to be a component in p/t binding by polymerases. Interestingly, the authors in Fedoroff et al. (*38*) proposed that more than four successive DNA bases are necessary to nucleate the B form in an A form RNA duplex. The switch to an overall more competent p/t substrate after six dNTPs are incorporated may reflect the ability of the p/t to switch from the classical RNA A form to the A-like to B conformation observed in the RT−p/t structure reported by Jacobo-Molina et al. (*29*).

In summary, binding and not catalytic properties of the initiation p/ts lead to the overall slow, nonprocessive polymerization rate during initiation. Analysis of the structural basis for the large differences seen between RNA- and DNA-primed transcription will be essential for the identification of inhibitors which specifically block the critical transition to the optimal DNA-primed activity.

ACKNOWLEDGMENT

We thank Karin Vogel-Bachmayr and Martina Wischnewski for excellent technical assistance, and Jochen Reinstein and John W. Erickson for fruitful discussions.

REFERENCES

1. Litvak, S., Sarih-Cottin, L., Fournier, M., Andreola, M., and Tarrago-Litvak, L. (1994) *Trends Biochem. Sci. 19*, 114−118.
2. Mak, J., and Kleiman, L. (1997) *J. Virol. 71*, 8087−8095.
3. Reardon, J. E., and Miller, W. H. (1990) *J. Biol. Chem. 265*, 20302−20307.
4. Oude Essink, B. B., Das, A. T., and Berkhout, B. (1996) *J. Mol. Biol. 264*, 243−254.
5. Isel, C., Lanchy, J.-M., Le Grice, S. F. J., Ehresmann, C., Ehresmann, B., and Marquet, R. (1996) *EMBO J. 15*, 917−924.
6. Ghosh, M., Williams, J., Powell, M. D., Levin, J. G., and Le Grice, S. F. (1997) *Biochemistry 36*, 5758−5768.
7. Isel, C., Marquet, R., Keith, G., Ehresmann, C., and Ehresmann, B. (1993) *J. Biol. Chem. 268*, 25269−25272.
8. Isel, C., Ehresmann, C., Keith, G., Ehresmann, B., and Marquet, R. (1995) *J. Mol. Biol. 247*, 236−250.
9. Lanchy, J. M., Ehresmann, C., Le Grice, S. F., Ehresmann, B., and Marquet, R. (1996) *EMBO J. 15*, 7178−7187.
10. Müller, B., Restle, T., Weiss, S., Gautel, M., Sczakiel, G., and Goody, R. S. (1989) *J. Biol. Chem. 264*, 13975−13978.
11. Milligan, J. F., Groebe, D. R., Witherell, G. W., and Uhlenbeck, O. C. (1987) *Nucleic Acids Res. 15*, 8783−8798.
12. Jeruzalmi, D., and Steitz, T. A. (1997) *J. Mol. Biol. 274*, 748−756.
13. Davanloo, P., Rosenberg, A. H., Dunn, J. J., and Studier, F. W. (1984) *Proc. Natl. Acad. Sci. U.S.A. 81*, 2035−2039.
14. Sambrook, J., Fritsch, E. F., and Maniatis, T. (1994) *Molecular Cloning*−*A Laboratory Manual*, Cold Spring Harbor Laboratory Press, Cold Spring Harbor, NY.
15. Divita, G., Müller, B., Immendörfer, U., Gautel, M., Rittinger, K., Restle, T., and Goody, R. S. (1993) *Biochemistry 32*, 7966−7971.
16. Krebs, R., Immendörfer, U., Thrall, S. H., Wöhrl, B. M., and Goody, R. S. (1997) *Biochemistry 36*, 10292−10300.
17. Kati, W. M., Johnson, K. A., Jerva, L. F., and Anderson, K. S. (1992) *J. Biol. Chem. 267*, 25988−25997.
18. Wöhrl, B. M., Krebs, R., Thrall, S. H., Le Grice, S. F. J., Scheidig, A. J., and Goody, R. S. (1997) *J. Biol. Chem. 272*, 17581−17587.
19. Rittinger, K., Divita, G., and Goody, R. S. (1995) *Proc. Natl. Acad. Sci. U.S.A. 92*, 8046−8049.
20. Jacobson, A. B., Good, L., Simonetti, J., and Zuker, M. (1984) *Nucleic Acids Res. 12*, 45−52.
21. Kerr, S. G., and Anderson, K. S. (1997) *Biochemistry 36*, 14056−14063.
22. Krebs, R. (1998) Ph.D. Thesis, University of Marburg, Germany.
23. Spence, R. A., Anderson, K. S., and Johnson, K. A. (1996) *Biochemistry 35*, 1054−1063.
24. Kerr, S. G., and Anderson, K. S. (1997) *Biochemistry 36*, 14064−14070.
25. Suo, Z., and Johnson, K. A. (1997) *Biochemistry 36*, 12459−12467.
26. Spence, R. A., Kati, W. M., Anderson, K. S., and Johnson, K. A. (1995) *Science 267*, 988−993.
27. Brautigam, C. A., and Steitz, T. A. (1998) *Curr. Opin. Struct. Biol. 8*, 54−63.
28. Kunkel, T. A., and Wilson, S. H. (1998) *Nat. Struct. Biol. 5*, 95−99.
29. Jacobo-Molina, A., Ding, J., Nanni, R. G., Clark, A. D., Lu, X., Tantillo, C., Williams, R. L., Kamer, G., Ferris, A. L., Clark, P., Hizi, A., Hughes, S. H., and Arnold, E. (1993) *Proc. Natl. Acad. Sci. U.S.A. 90*, 6320−6324.
30. Doublié, S., Tabor, S., Long, A. M., Richardson, C. C., and Ellenberger, T. (1998) *Nature 391*, 251−258.
31. Kiefer, J. R., Mao, C., Braman, J. C., and Beese, L. S. (1998) *Nature 391*, 304−307.
32. Steitz, T. A. (1990) *Q. Rev. Biophys. 23*, 205−280.
33. Bebenek, K., Beard, W. A., Darden, T. A., Li, L., Prasad, R., Luton, B. A., Gorenstein, D. G., Wilson, S. H., and Kunkel, T. A. (1997) *Nat. Struct. Biol. 4*, 194−197.
34. Saenger, W. (1984) *Priciples of Nucleic Acid Structure*, Springer-Verlag New York.
35. Salazar, M., Fedoroff, O. Y., Miller, J. M., Ribeiro, N. S., and Reid, B. R. (1993) *Biochemistry 32*, 4207−4215.
36. Horton, N. C., and Finzel, B. C. (1996) *J. Mol. Biol. 264*, 521−533.
37. Gyi, J. I., Lane, A. N., Conn, G. L., and Brown, T. (1998) *Biochemistry 37*, 73−80.
38. Fedoroff, O. Y., Salazar, M., and Reid, B. R. (1993) *J. Mol. Biol. 233*, 509−523.

BI981102T